

Spectral phase optimization of femtosecond laser pulses for narrow-band, low-background nonlinear spectroscopy

Vadim V. Lozovoy, Janelle C. Shane, Bingwei Xu and Marcos Dantus
Department of Chemistry and Department of Physics and Astronomy, Michigan State University,
East Lansing, MI 48824, USA
dantus@msu.edu

Abstract: We use experimental search space mapping to examine the problem of selective nonlinear excitation with binary phase shaped femtosecond laser pulses. The search space maps represent a graphical view of all the possible solutions to the selective nonlinear excitation problem along with their experimental degrees of success. Using the information learned from these maps, we generate narrow lines with low background in second harmonic generation and stimulated Raman scattering spectra.

© 2005 Optical Society of America

OCIS codes: (320.7110) Ultrafast nonlinear optics; (320.5540) Pulse shaping

References and Links

1. A. M. Weiner, D. E. Leaird, G. P. Wiederrecht, and K. A. Nelson, "Femtosecond Pulse Sequences Used for Optical Manipulation of Molecular-Motion," *Science* **247**, 1317-1319 (1990).
2. Z. Zheng, and A. M. Weiner, "Coherent control of second harmonic generation using spectrally phase coded femtosecond waveforms," *Chem. Phys.* **267**, 161-171 (2001).
3. D. Meshulach, and Y. Silberberg, "Coherent quantum control of two-photon transitions by a femtosecond laser pulse," *Nature* **396**, 239-242 (1998).
4. D. Oron, N. Dudovich, and Y. Silberberg, "Femtosecond phase-and-polarization control for background-free coherent anti-Stokes Raman spectroscopy," *Phys. Rev. Lett.* **90**, 213902 (2003).
5. J. M. Dela Cruz, I. Pastirk, V. V. Lozovoy, K. A. Walowicz, and M. Dantus, "Multiphoton intrapulse interference 3: Probing microscopic chemical environments," *J. Phys. Chem. A* **108**, 53-58 (2004).
6. H. A. Rabitz, M. M. Hsieh, and C. M. Rosenthal, "Quantum optimally controlled transition landscapes," *Science* **303**, 1998-2001 (2004).
7. M. Comstock, V. V. Lozovoy, I. Pastirk, and M. Dantus, "Multiphoton intrapulse interference 6; binary phase shaping," *Opt. Express* **12**, 1061-1066 (2004).
8. K. A. Walowicz, I. Pastirk, V. V. Lozovoy, and M. Dantus, "Multiphoton intrapulse interference. 1. Control of multiphoton processes in condensed phases," *J. Phys. Chem. A* **106**, 9369-9373 (2002).
9. V. V. Lozovoy, I. Pastirk, K. A. Walowicz, and M. Dantus, "Multiphoton intrapulse interference. II. Control of two- and three-photon laser induced fluorescence with shaped pulses," *J. Chem. Phys.* **118**, 3187-3196 (2003).
10. I. Pastirk, J. M. Dela Cruz, K. A. Walowicz, V. V. Lozovoy, and M. Dantus, "Selective two-photon microscopy with shaped femtosecond pulses," *Opt. Express* **11**, 1695-1701 (2003).
11. V. V. Lozovoy, and M. Dantus, "Systematic control of nonlinear optical processes using optimally shaped femtosecond pulses," *Chem. Phys. Chem.* **6**, 1952-1967 (2005).
12. A. M. Weiner, "Femtosecond pulse shaping using spatial light modulators," *Rev. Sci. Instrum.* **71**, 1929-1960 (2000).
13. V. V. Lozovoy, I. Pastirk, and M. Dantus, "Multiphoton intrapulse interference. IV. Ultrashort laser pulse spectral phase characterization and compensation," *Opt. Lett.* **29**, 775-777 (2004).
14. B. Xu, J. M. Gunn, J. M. DelaCruz, V. V. Lozovoy, and M. Dantus, "Quantitative investigation of the MIIPS method for phase measurement and compensation of femtosecond laser pulses," *J. Opt. Soc. Am. B*, in press.
15. V. V. Lozovoy, B. Xu, J. C. Shane, and M. Dantus, "Selective nonlinear excitation with pseudorandom Galois fields," to be published (2005).
16. J. M. Dela Cruz, I. Pastirk, M. Comstock, V. V. Lozovoy, and M. Dantus, "Use of coherent control methods through scattering biological tissue to achieve functional imaging," *P. Natl. Acad. Sci. USA* **101**, 16996-17001 (2004).
17. I. Pastirk, M. Kangas, and M. Dantus, "Multidimensional analytical method based on binary phase shaping of femtosecond pulses," *J. Phys. Chem. A* **109**, 2413-2416 (2005).

1. Introduction

The ability to produce a narrow tunable peak in the nonlinear spectra of a femtosecond laser would allow nonlinear optical processes such as two-photon excitation and impulsive stimulated Raman excitation to be controlled with a single femtosecond source. Approaches guided empirically and by theory have shown remarkable progress toward this goal [1-5]. It is important not only to be able to generate a strong signal at a desired wavelength (Fig. 1(a), but also to suppress background elsewhere in the nonlinear spectra (Fig. 1(b), the latter being the goal of this project.

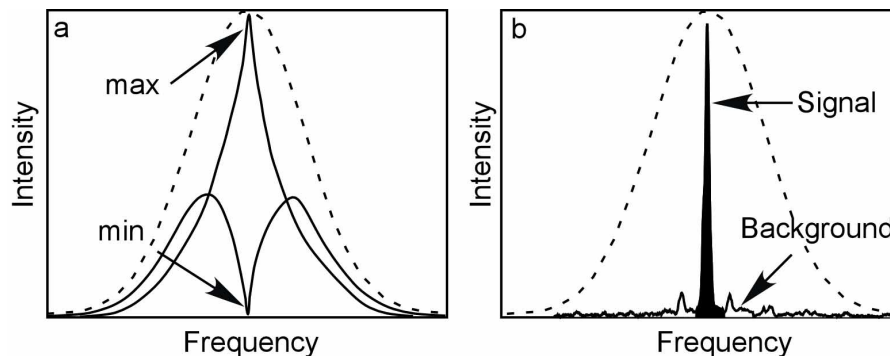


Fig. 1. Nonlinear spectra of phase modulated pulses. The dashed line is the spectrum of a Gaussian transform-limited (flat spectral phase) pulse. (a) Maximization or minimization of nonlinear spectra at a selected frequency. (b) Generation of a narrow peak at a selected frequency with low background (the goal of this project).

The primary obstacle to achieving this goal is the difficulty of finding the femtosecond pulse shape that produces the desired nonlinear spectra. The success of a search method such as a genetic algorithm depends largely on the nature of the search space, or the distribution of good solutions over the set of all possible pulse shapes. In the ideal case of infinitely precise control of a pulse's shape and the absence of experimental noise, the search space for a given nonlinear process is convex, meaning that each possible pulse shape can be transformed into a slightly better pulse shape by an infinitesimally small change to just one parameter, allowing the best possible pulse shape (the global maximum) to be quickly reached through a series of small changes [6]. However, the current method of controlling a pulse's shape, the spatial light modulator (SLM), can provide only a finite number of possible pulse shapes, usually about 100 SLM pixels (N), 1000 reliable phase values (N_ϕ), and 1000 reliable amplitude values (N_A). The set of possible pulse shapes is no longer continuous, and therefore the search space is no longer convex. Instead of an easy path toward the optimum solutions, we have dead-end solutions called local maxima, which are suboptimal but must be dramatically changed to reach a better solution. Under experimental conditions, the huge number of variables makes the search for an optimal pulse shape a daunting task; the number of pulse shapes possible using the SLM described above is $(N_\phi \times N_A)^N = 10^{600}$. A search space this size makes all but the most convex problems extremely difficult.

Our approach to the problem of creating a narrow peak in nonlinear spectra is to reduce the number of variables to make the problem more manageable, while making sure not to eliminate all the best solutions from the search space. To do this, we must eliminate redundancy while preserving control over the parts of a pulse shape that contribute to our

desired nonlinear effects. We have shown that the use of binary phase shaping [7], in which no amplitude shaping is used and the only two values of spectral phase allowed are 0 or π , allows us to reduce the problem to that of constructive and destructive interference between frequencies [8-10]. The search space becomes not only dramatically smaller but also more readily analyzable and, as we will show, amenable to search space mapping.

In this paper, we examine the distribution of the binary phase functions that best create narrow peaks at desired locations in the nonlinear spectra. The two-dimensional plot of these distributions are called search space maps, and from them we can observe symmetry rules that agree with theoretical predictions [11]. Using the information provided by search space mapping, we explore a subset of 48-bit functions through simulation and experimental verification, and demonstrate tunable narrow peaks.

2. Experimental section

We measured second harmonic generation (SHG) and simulated Raman scattering (SRS) spectra of pulses from a Ti:Sapphire oscillator (K&M Laboratories) capable of producing 10 fs pulses (110 nm FWHM) centered near 800 nm. The average power of the oscillator was 250 mW, with a repetition frequency of 97 MHz. The beam went through a folded pulse compressor consisting of a pair of SF10 prisms and then into a pulse shaper. The pulse shaper, consisting of a SF10 and a BK7 prism, a 200-mm focal length cylindrical mirror, and a dual-mask SLM (CRI, Inc., SLM-256), is based on the general design of Weiner [12] in the folded geometry. To achieve accurate phase retardations, each pixel of the SLM was carefully calibrated by measuring the polarization-dependent transmission of light through each pixel. The multi-photon intra-pulse interference phase scan (MIIPS) method [13, 14] was used for all the experiments to achieve TL pulses at the target within 0.05 radian precision. For SHG experiments, the beam was focused on a 10 μm β -BBO type I crystal and the signal was recorded with a spectrometer of spectral resolution ~ 0.3 nm. For SRS experiments, the beam was introduced into a balanced Michelson interferometer (FR-103PD, Femtochrome Research, Inc). SRS spectra were retrieved from Fourier transformation of autocorrelation traces obtained by a two-photon diode. Acquisition of a single spectrum requires 0.8 s for SHG and 4 s for SRS; therefore, the 65,536-phase mapping experiments described below lasted 15 hours for SHG and 70 hours for SRS. Significant speedup of acquisition times is possible, for example through use of a single pulse autocorrelator.

3. Results and discussion

3.1 Mapping of exhaustive experimental evaluation

In the first series of experiments we investigated all possible 16-bit binary phase functions for their ability to generate selective SHG and SRS excitation. We applied each phase to the center spectral region of our femtosecond laser pulses, using amplitude shaping to eliminate the signal outside of this spectral window. Each of the 16 logical bits covered 4 SLM pixels for SHG and 3 SLM pixels for SRS. For both SHG and SRS, we defined a window of spectral width 1.3 nm or 50 cm^{-1} ; the integrated intensity of the spectrum inside this window was defined as signal S, while the integrated intensity of the spectrum outside the window was defined as background B (Fig. 1). For SRS, we disregarded the spectral region below 150 cm^{-1} , a region that is essentially unaffected by phase shaping. We assigned each phase function a fitness value S/B based on the ratio between integrated signal and integrated background.

To visualize the search space, we transformed each binary phase function into an (x,y) coordinate on a two-dimensional plot called a search space map. We first translated each binary phase function (for example, $\pi 0 \pi \pi 0 0 0 0 0 \pi 0 0 \pi \pi \pi 0$) into a binary sequence (1011000001001110₂ in this example), then divided this sequence into two halves (x = 10110000₂, y = 01001110₂). The binary x- and y-halves of the sequence were directly converted to their base-10 equivalents (x = 13₁₀, y = 114₁₀). The resulting (x,y) coordinate pair corresponds to a point on a 2D map, which is assigned a color based on the experimental

performance of the original binary phase function; red if the S/B value was high, down to black for a very low S/B. For the SHG search space maps, the x portion (first half) of the binary sequence was reversed before conversion to decimal. We applied this reversal to highlight the different roles of symmetry in SHG as opposed to SRS, as discussed below.

Figure 2 shows experimental SHG and SRS search spaces for signal windows placed in the middle of the available nonlinear spectra. The binary phase sequence with the highest S/B ratio for SHG is $\pi 0 \pi \pi 0 \pi \pi \pi 0 0 0 \pi 0 0 \pi \pi$, which is mapped to (237,19) as described above, while the binary phase sequence with the highest S/B ratio for SRS is $\pi 0 \pi \pi 0 0 0 0 0 \pi 0 0 \pi \pi \pi 0$, mapped to (13,114).

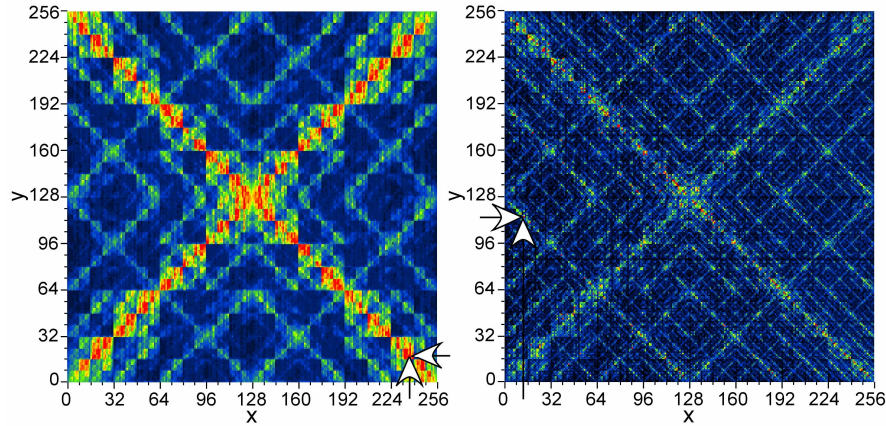


Fig. 2. Experimental mapping of selective SHG (left) and SRS (right) at the center of the spectrum (see Fig. 1(b)). X and y coordinates are the decimal representations of the left and right halves of the binary phase sequences, respectively, and color as z coordinate is the experimentally measured signal to background ratio of nonlinear excitation. Here, phase sequences with high S/B ratios are shown in red, while sequences with low S/B ratios are shown in black. Arrows point to the locations of the global maxima.

Many of the good phase functions (shown in red) are found on the lines $y=x$ and $y=x_{\max}-x$. For the SHG maps, these lines contain only phase functions that are reflection symmetric or antisymmetric about Ω ; that is, $\phi_{SHG}(\Omega+\omega)=\pm\phi_{SHG}(\Omega-\omega)$, while for SRS the phases on these lines have translation symmetry or anti-symmetry about Ω ; that is, $\phi_{SRS}(\omega)=\pm\phi_{SRS}(\Omega+\omega)$. These lines are dominant features on the search space maps, agreeing with theoretical predictions of the role of symmetry in constructing phase functions for optimizing nonlinear optical processes [11]. Note that even among symmetric phases on the search space map lines, there are phases with poor S/B ratios. To achieve the best S/B ratios among symmetric phases one half of the binary phase function, $\phi_{SHG}(\Omega+\omega)$ or $\phi_{SRS}(\omega)$, must contain a pseudorandom series of bit flips [15].

As the target signal wavelength is scanned across the nonlinear spectrum, the center of symmetry that maximizes this signal is scanned across the phase function. Movie 1 and movie 2 show the SHG or SRS maps when signal window is scanned from one end of the spectrum to the other. In each case, the phase functions with the highest S/B ratios are located on lines that contain only symmetric or antisymmetric phases, with the locations of the lines changing to reflect the changing location of the center or symmetry.

3.2 Experimental scanning of narrow peaks in SHG and SRS spectra

As we can see from the previous experiment, the best solutions belong to the class of symmetrical phase functions, which in general have a much higher concentration of good solutions than any other class of phase functions. Given this distribution of good solutions in the search space, we decided to focus our efforts on symmetric phase functions in a second set of experiments designed to explore optimization using a larger number of pixels. We

explored symmetric 48-bit sequences, of which there are $2^{48/2}$ or roughly 16 million. To further reduce this search space size, we used a 5-bit region of constant phase in $\phi_{SHG}(\Omega + \omega)$ or $\phi_{SRS}(\omega)$. This reduces the number of possible sequences to $2^{48/2-5}$, about half a million.

We examined not only phase functions to optimize nonlinear signal at the center of the spectrum produced by a TL pulse, but also functions that optimized signal at other locations in the nonlinear spectra. Symmetry provides maximization of the signal at a selected frequency. When this frequency is detuned from the center of the spectrum, the required center of symmetry is detuned as well, resulting in SLM pixels at the far end of the spectrum that do not contribute to the symmetry. These extra pixels only contribute to background, so for our experiments we eliminated signal from these locations using amplitude shaping.

The best results from the exhaustive search above were evaluated using a sophisticated simulation program that took into account all major experimental effects contributing to the final appearance of SRS and SHG spectra, with the best-performing phase functions then evaluated in the laboratory. Figure 3 shows the excellent agreement between simulation and experiment. To achieve this close agreement, our simulation accounts for four main effects: the spectrum of the fundamental pulse (shown in red in Fig. 3(a,b), the nonlinear dispersion of the pulse in the frequency domain at the shaper, limited spectral resolution of the SLM, and the temporal resolution of the interferometer used for the SRS measurements.

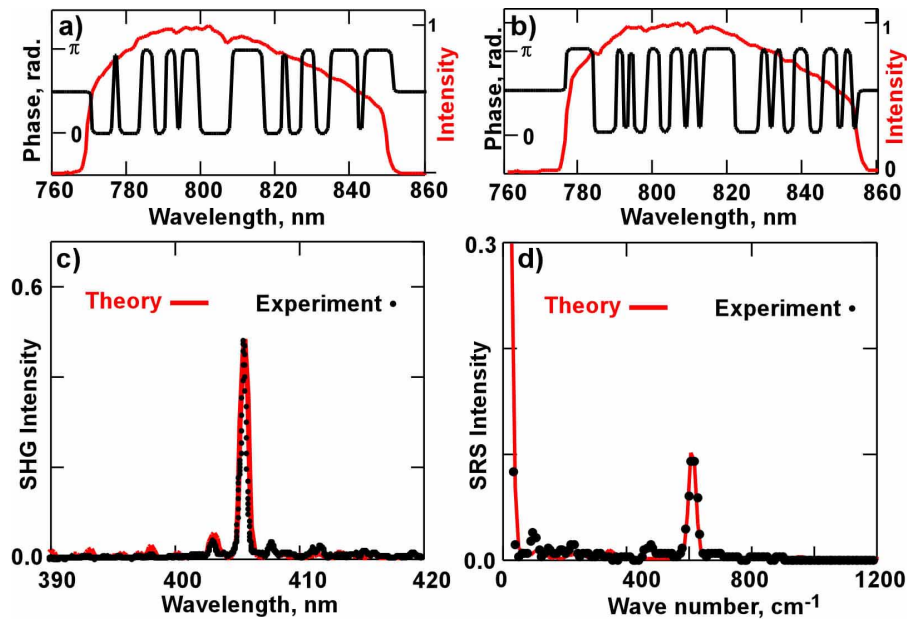


Fig. 3. Experimental generation (dots) and simulation (red) of narrow-band and low-background nonlinear fields using optimized binary phase functions. (a) and (b) Phase (black) and amplitude (red) modulation was imprinted with the SLM on a broad fundamental pulse. (c) SHG spectrum measured with a nonlinear crystal. (d) SRS spectrum recorded as the Fourier transform of the autocorrelation trace using a collinear Michelson interferometer.

Experimental signals were found to have one half or one third of the theoretically possible amplitude for SHG and SRS, respectively. The observed spectral width was about 0.8 nm and 60 cm^{-1} for SHG and SRS spectra, respectively. These values are about 1.5 times broader than their ideal limit, the spectral width of one pixel in the SLM. We attribute amplitude and resolution losses to the spectral resolution of the shaper and the nonlinear spectral dispersion. Through exhaustive search of symmetric 48-pixel phase functions, we were able to find a set of shaped pulses that can be used to scan a narrow-band nonlinear excitation over a wide spectral range in SHG and SRS spectra, as shown in Movies 3 and 4. The spectral range of scanning depends on the spectral width of the fundamental pulse. Most

importantly, the S/B ratio was about 4 over a very broad spectral range. Using 48 pixels we have substantially suppressed the background, as predicted in [11, 15].

The ultimate goal for our shaped pulses is to apply them to a source producing ultrabroad bandwidth. The bandwidth of modern lasers with chirped mirrors or from continuum generation in fibers would allow spectral tuning from 300 to 550 nm for the two photon field and up to 5000 cm^{-1} for Raman scattering. Using a 640-pixel shaper with optical resolution of one pixel will improve the resolution down to few wave numbers and essentially eliminate the background.

Reaching single wave-number spectral resolution over a broad tuning range is not an easy task, even from a theoretical point of view. Exhaustive search is impossible with the large number of pixels required, and the non-convex nature of the search space presents a serious challenge to optimization attempts using genetic algorithms. As we demonstrated above, reducing the search space by restricting our search to binary symmetric sequences dramatically reduced the evaluation time required, while still allowing us to reach excellent solutions. The 48-pixel search space was reduced from 10^{288} for pulses with unrestricted amplitude and phase values to about 10^6 for binary symmetric phases, a reduction of several hundred orders of magnitude. Search space reduction on this scale can mean the difference between an intractable problem and one that can be solved through exhaustive evaluation or a genetic algorithm optimized to work on the further reduced binary search space. We are currently investigating further methods for search space reduction among symmetric binary phases.

4. Conclusion

We have shown that search space reduction is a powerful way to deal with the non-ideal nature of experimental conditions. We reduced the nonlinear control problem of producing a narrow tunable peak in SHG and SRS spectra to the barest essentials and produced a map of this reduced search space. We discovered through simulation and experimental confirmation that the spectral resolution attainable is limited by the resolution of the shaper used and that scanning range is limited only by the spectral range of the initial femtosecond pulse. Genetic algorithm search of a further reduced search space will allow the use of a shaper with several hundred pixels to achieve Raman spectral resolution of few wave numbers. A potential advantage of nonlinear optical spectroscopy using shaped pulses is the possibility of replacing two tuned and phase synchronized lasers for coherent anti-Stokes Raman spectroscopy with one ultra-broadband femtosecond laser and shaper. For optical heterodyne four wave mixing, four coherent optical fields contribute to the signal, which will provide even better signal to background ratio when optimal shaping is used. Beyond selective two-photon processes, the exhaustive evaluation of reduced binary search spaces has proven to be a valuable and practical approach toward finding optimal phase shape pulses to be used in functional imaging through biological tissue [16], gaining multidimensionality in analytical chemistry [17], and identifying and quantifying mixtures of isomeric compounds [18].

Acknowledgments

We gratefully acknowledge funding for this research from the Chemical Sciences, Geosciences and Biosciences Division, Office of Basic Energy Sciences, Office of Science, U.S. Department of Energy. We are also thankful to Professor Erik Goodman for insightful discussions on search space reduction.